targets

MDPI

Article

Requirements of Constrictive Binding and Dynamic Systems on Molecular Cages for Drug Delivery

Giovanni Montà-González [1,2], Ramón Martínez-Máñez [1,2,3,4,5,*] and Vicente Martí-Centelles [1,2,3,*]

[1] Instituto Interuniversitario de Investigación de Reconocimiento Molecular y Desarrollo Tecnológico (IDM), Universitat Politècnica de València, Universitat de València, Camino de Vera s/n, 46022 Valencia, Spain; gmongon@upv.es
[2] Departamento de Química, Universitat Politècnica de València, Camino de Vera s/n, 46022 Valencia, Spain
[3] CIBER de Bioingeniería Biomateriales y Nanomedicina, Instituto de Salud Carlos III, 28029 Madrid, Spain
[4] Unidad Mixta de Investigación en Nanomedicina y Sensores, Universitat Politècnica de València, Instituto de Investigación Sanitaria La Fe (IISLAFE), Avenida Fernando Abril Martorell 106, 46026 Valencia, Spain
[5] Unidad Mixta UPV-CIPF de Investigación en Mecanismos de Enfermedades y Nanomedicina, Universitat Politècnica de València, Centro de Investigación Príncipe Felipe, Avenida Eduardo Primo Yúfera 3, 46012 Valencia, Spain
* Correspondence: rmaez@qim.upv.es (R.M.-M.); vimarce1@upv.es (V.M.-C.)

Abstract: Molecular cages have promising host–guest properties for drug delivery applications. Specifically, guest⊂cage complexes can be used for the on-command release of encapsulated guest molecules in response to specific stimuli. This research explores both the dynamic and constrictive binding guest⊂cage systems for drug encapsulation and release in biological environments. In dynamic systems, the guest rapidly passes in-and-out through the portals of the cage, enabling drug delivery in vitro but facing limitations in vivo due to dilution effects that result in guest release. These challenges are addressed by constrictive binding systems, where the guest is trapped in a "gate-closed" state within the cage. In these systems, the on-command release is triggered by a "gate opening" event, which lowers the guest–out energy barrier. A full guest release is achieved when the gate opening reduces the cage–guest affinity, making constrictive binding systems more effective for controlled drug delivery. As a result, this study shows that guest⊂cage complexes have suitable properties for drug delivery in biological contexts.

Keywords: molecular cages; supramolecular chemistry; metal–organic cages; organic cages; drug delivery; host–guest chemistry

check for updates

Citation: Montà-González, G.; Martínez-Máñez, R.; Martí-Centelles, V. Requirements of Constrictive Binding and Dynamic Systems on Molecular Cages for Drug Delivery. *Targets* **2024**, 2, 372–384. https://doi.org/10.3390/targets2040021

Academic Editor: Huangxian Ju

Received: 30 September 2024
Revised: 30 October 2024
Accepted: 15 November 2024
Published: 19 November 2024

Copyright: © 2024 by the authors. Licensee MDPI, Basel, Switzerland. This article is an open access article distributed under the terms and conditions of the Creative Commons Attribution (CC BY) license (https://creativecommons.org/licenses/by/4.0/).

1. Introduction

Molecular cages are supramolecular structures that can isolate guest molecules from the surrounding media via encapsulation in their central cavity, mimicking the encapsulation processes found in biological systems [1–3]. In fact, in biology, compartmentalization has vital importance in keeping living organisms away from equilibrium, resulting in a complex network of non-equilibrium chemical systems [4]. Molecular cages are therefore suitable systems for mimicking these complex functions. The three-dimensional shape of their cavity gives a unique preorganization with an enhanced affinity for guests in comparison to related supramolecular architectures such as macrocycles [5–7]. This property makes cages unique species for diverse applications such as catalysis [8–12], the sensing of diverse chemical species [13–18], the separation of chemicals [19–23], the removal of pollutants from water [24–27], the stabilization of chemical species [28,29], biological applications [30–39], and many others [1,2]. In addition to these properties, molecular cages can be engineered to transport cargo molecules [40] with stimuli-responsive properties to pH [35,41,42] and light [43–46], among others [47–52]. Typically, cages are prepared by the thermodynamically controlled self-assembly of metals and ligands to yield metallo-cages

or by the self-assembly of only organic ligands to yield pure organic cages [1,2,53–55]. To facilitate the design of cages with specific geometries and properties, computational modeling has been extensively used. This allows for reducing trial-and-error attempts or predicting host–guest properties [56–62].

Focusing on the therapeutic applications of molecular cages, cages are capable of encapsulating drugs, forming inactive guest⊂cage complexes, in which the activity of the drug is restored upon their release from the cage [30,31]. In this area, it is crucial to design cages that efficiently encapsulate drugs and respond to selective stimuli for controlled drug release [33,63,64]. Various systems have been developed for this purpose, most of which rely on equilibrium processes, which present limitations related to dynamic equilibria and drug dissociation when applied in a physiological environment [1,2]. Achieving systems where drugs are kinetically trapped inside the cage is a challenging task. To accomplish this, the constrictive binding strategy has been proposed in simple host–guest systems, where the guest in–out activation barrier prevents rapid equilibrium between the drug inside the cavity and the external environment. The in-and-out passage of the guest molecule requires heating to widen the portals to create sufficient space [65].

Cram, back in 1991, reported an example of the constrictive binding of a 1,1,2,2-tetrachloroethane guest molecule using a fully organic hemicarcerand host **C1** (Figure 1a) [66]. This guest⊂cage complex was stable at room temperature in the solid state or in solution, but was slowly decomplexed by heating it at 100–134 °C. A van't Hoff analysis provided an activation barrier of 24.6 kcal/mol, with a $t_{1/2}$ value of 18 h at 100 °C. Further studies by Cram showed that the in–out activation barriers were guest-dependent for a series of hemicarcerands, with the larger guests found to have lower activation energies for decomplexing. This is likely due to the increased compression of the cage to accommodate them, which were released upon decomplexation [67]. The relative size of the guest regarding the size of the portals of the cage was a key parameter for successful constrictive binding. If the guests were too small, constrictive binding was ineffective, as the guest molecules passed through the portals; if the guests were too large, the energy barrier became too high, preventing complexation from occurring [68,69]. Both the guest shape and size influenced the observed constrictive binding [70]. As a result, the in-and-out kinetics of the guest depended on the cage's conformation and was also correlated with the cage–guest affinity, where stronger affinity led to slower kinetics [71]. The binding properties in these guest⊂cage complexes can be described as the combination of intrinsic binding (i.e., free energy difference between the complex and free cage and guest) and constrictive binding, as the additional free energy barrier was associated with the guest passing through the portals of the cage (Figure 1b) [72]. These systems, in which the guest molecule is trapped inside the cage and is only released from it under specific conditions, act as a gating mechanism [72–80].

Cages **C2**–**C4** showed specific examples of gating mechanisms that resulted in guest release in response to specific stimuli (Figure 2). Cage **C2** features a photoswitchable gate based on the reversible dimerization of anthracene. Irradiation at 350 nm produces gate closing via the dimerization reaction, and irradiation at 254 nm (or heating at 60 °C) produces gate opening by breaking the dimer. Cage **C2** was tested with *p*-dimethoxybenzene, *o*-xylene, *m*-xylene, *p*-xylene, anisole, 4-methylanisole, 1,1,2,2-tetrachloroethane, and 1,1,2,2-tetrabromoethane. The authors proved that the *p*-dimethoxybenzene⊂**C2** complex was stable in the dark at room temperature for more than 4 weeks without any detectable guest release [74]. Cage **C3** had a gate formed with a nitrobenzyl ether group. Gate opening took place via irradiation at 330 nm, producing irreversible C–O bond cleavage, resulting in the guest (dimethylacetamide or N-methyl-2-pyrrolidinone) escaping from the cavity [75]. Cage **C4** featured a reversible redox-controllable disulfide gate that was closed when the disulfide bridge was intact and opened upon the conversion of the disulfide to dithiol. Gate opening occurred via a reaction with a thiol (such as dithiothreitol or $HS(CH_2)_4SH$) in the presence of a base (DBU), leading to the release of guests from the cavity, including

2-bromo-1,4-dimethoxybenzene, 1,2,3-trimethoxybenzene, and *tert*-butylbenzene, and gate closing was achieved by a reaction with iodine and triethylamine [76,77].

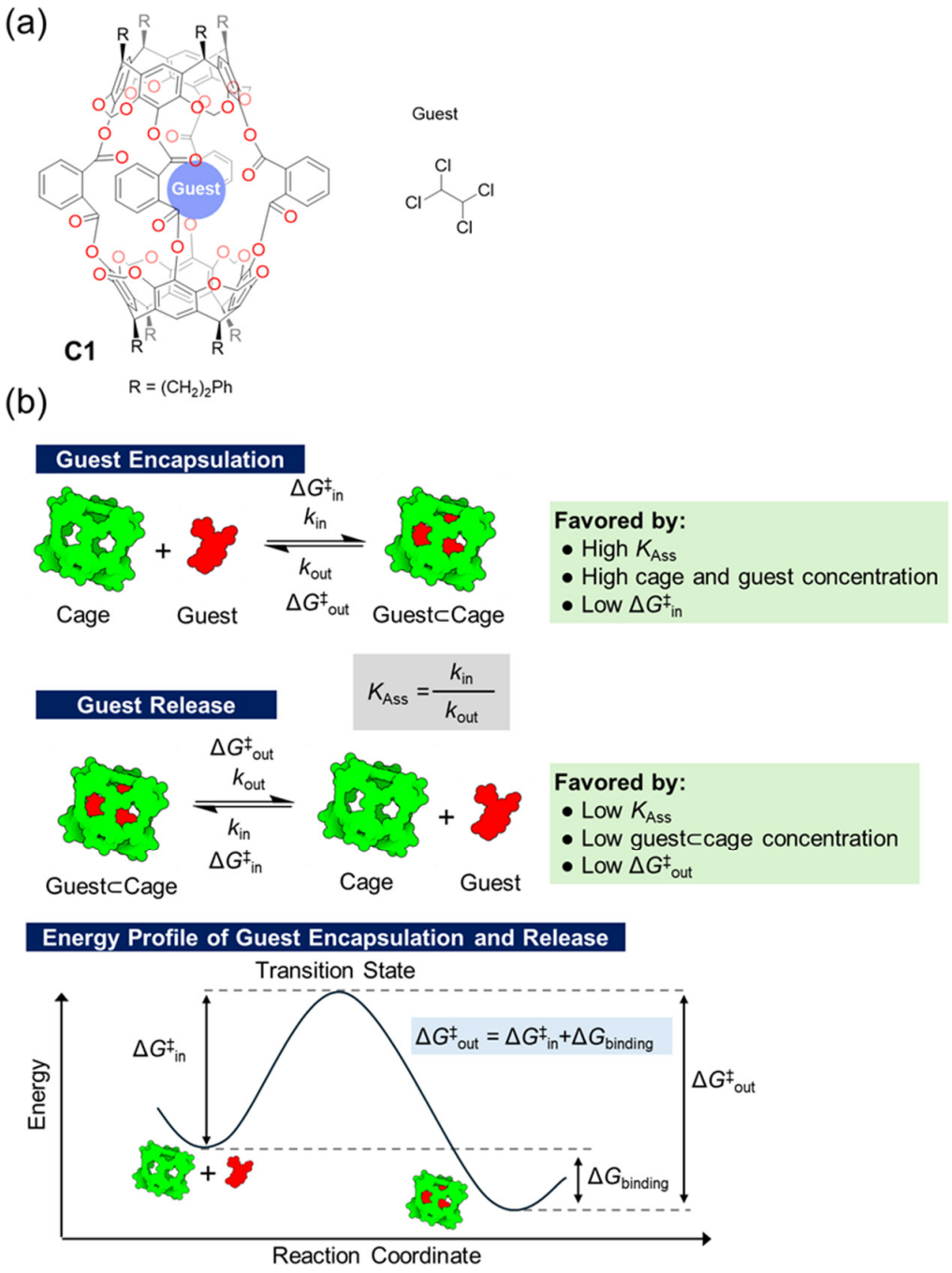


Figure 1. (**a**) A constrictive binding hemicarcerand host **C1** reported by Cram in 1991. (**b**) A schematic representation of the encapsulation of a guest molecule driven by the association constant of the guest into the molecular cage followed by the corresponding guest release. The equilibrium shifted to the formation of the guest⊂cage complex or the release of the guest depending on the concentration, association constant, and energy barriers. The energy profile of both the guest encapsulation and release is also shown.

Metallo-organic cages have the same host–guest behavior as organic cages. Fujita and his team have shown a "ship in a bottle" entrapment-type synthesis using cage **C5,** showing that a large labile cyclic silanol that fits tightly to the cage cavity prevents its hydrolysis for more than one month (Figure 3) [81]. This shows the feasibility of using molecular cages to

effectively isolate the encapsulated guest from the surrounding media, highlighting the importance of having a large-enough-sized guest that cannot pass through the portals of the host. If the size of the guest is smaller than the portal, Raymond showed that the partial dissociation of the cage host structure **C6** could create a portal for in–out guest passage, and the deformation of the host structure could create a dilated aperture for guest passage without any host rupture. Smaller guests, such as NMe_4^+, NEt_4^+, and $CoCp_2^+$, exhibited faster in–out rates. In contrast, the larger $CoCp^*{}_2^+$ showed significantly slower in–out rates (Figure 3) [82]. Nitschke and his team measured the rate constant for guest uptake (k_{in}) and the association constant (K_{Ass}) for Nitschke's water-soluble Fe_4L_6 metal–organic cage **C7**. We have carefully reanalyzed these data and determined the guest release rate constants (k_{out}) as $k_{out} = k_{in}/K_{Ass}$, showing a guest release decrease with the guest size. On one side, the guest must have a smaller size than the cavity size (150 Å^3) as guests with a size of 135 Å^3 or larger do not bind. For smaller guests, the k_{out} decreases with the size of the guest, from 5 $\times 10^{-2}$ s^{-1} for acetone (73 Å^3) to 5 $\times 10^{-8}$ s^{-1} for cyclohexane (111 Å^3). These results show an impressive change of six orders of magnitude in the out-rate, changing the release timescale from seconds to months, from the smaller to the larger guest (Figure 3) [69].

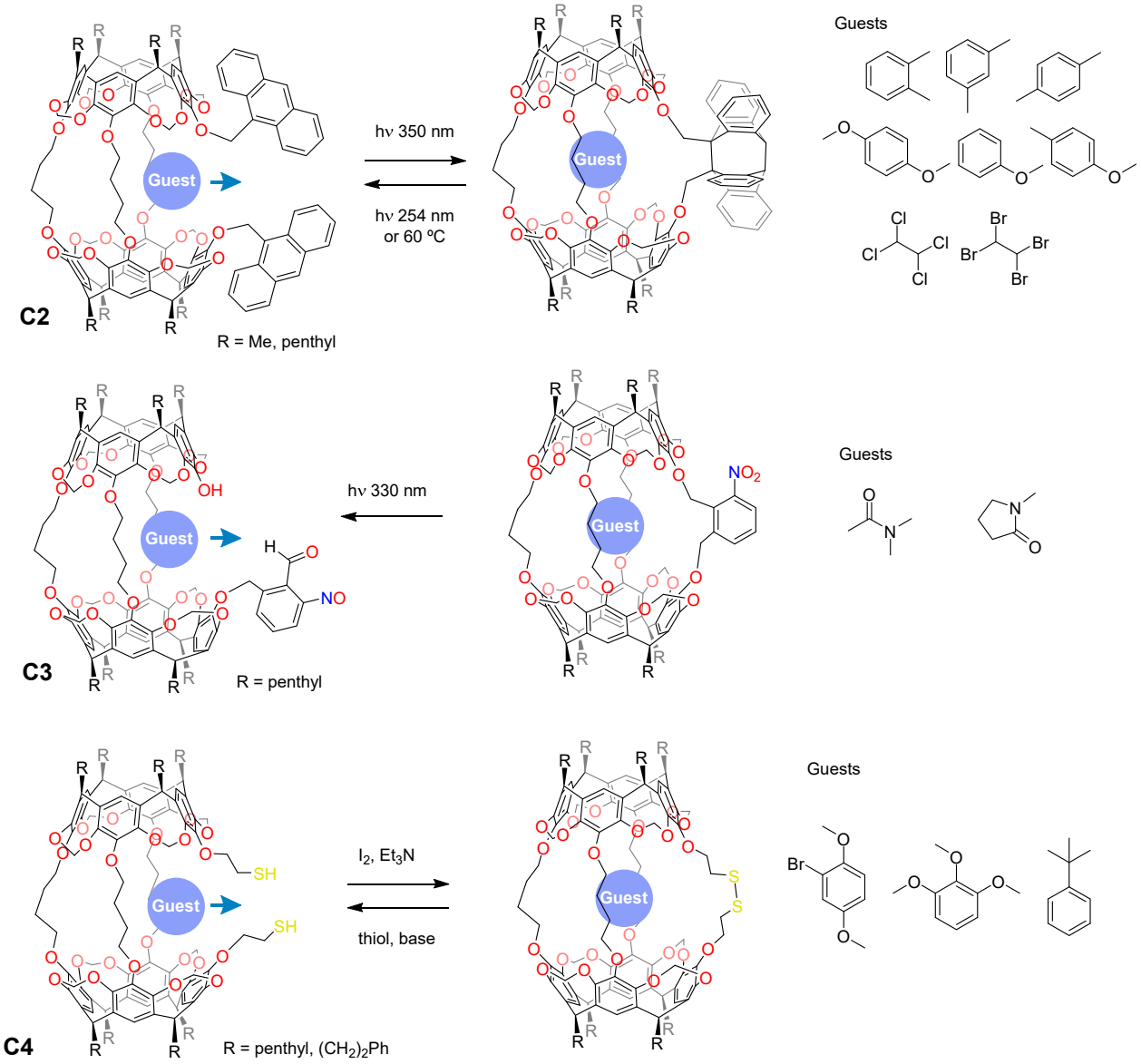


Figure 2. Examples of guest⊂cage complexes with molecular gates with fully organic cages **C2**–**C4**.

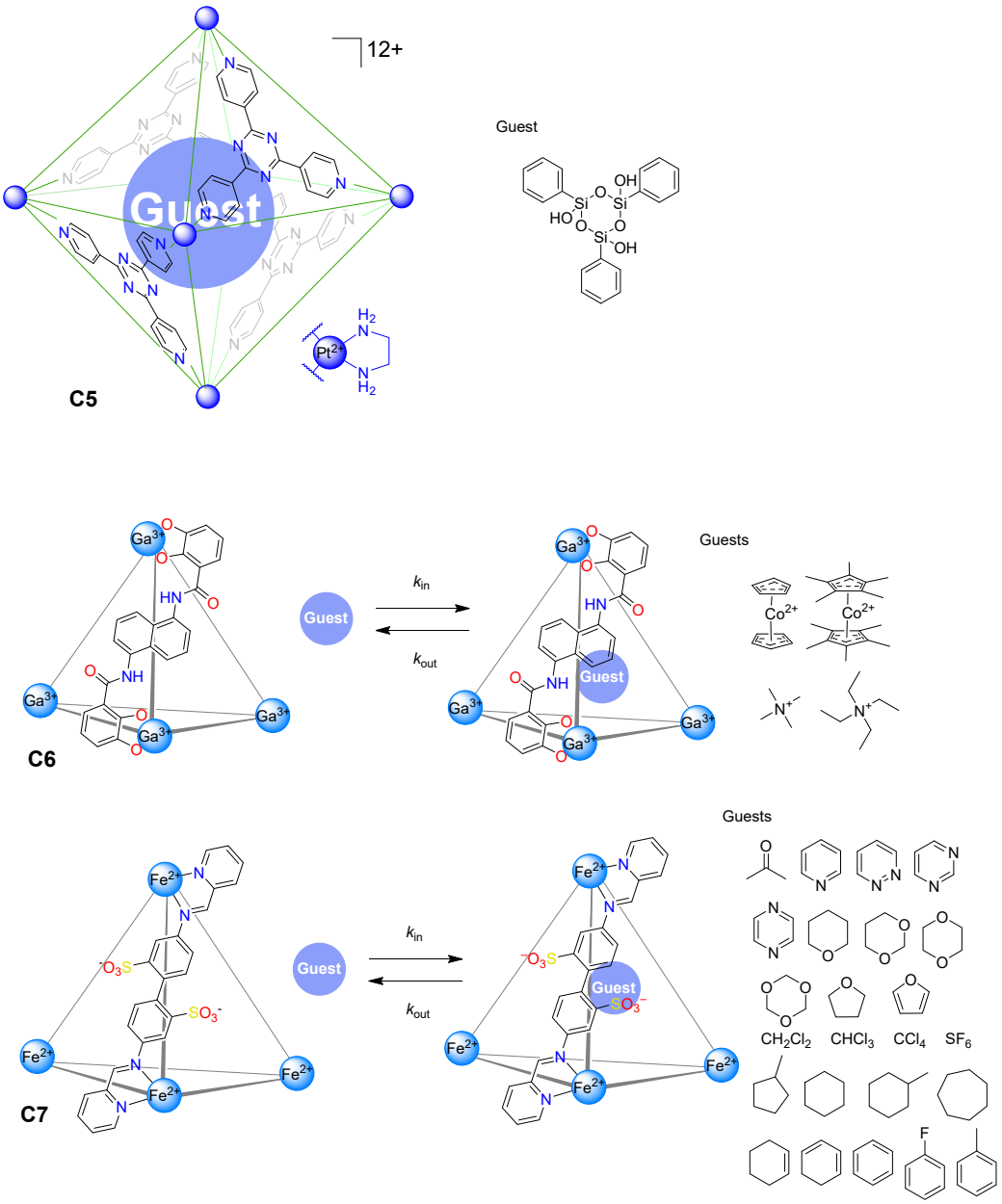


Figure 3. Examples of guest⊂cage complexes with metallo-organic cages **C5**–**C7**, showing guests with varying in–out exchange rates.

In this work, we studied the thermodynamic and kinetic requirements of guest⊂cage complexes for drug delivery applications. We focused on both dynamic and constrictive binding systems, analyzing the effects of dilution, binding constant strength, and the activation energy required for the encapsulated guest to escape the cavity of the cage in the operational systems.

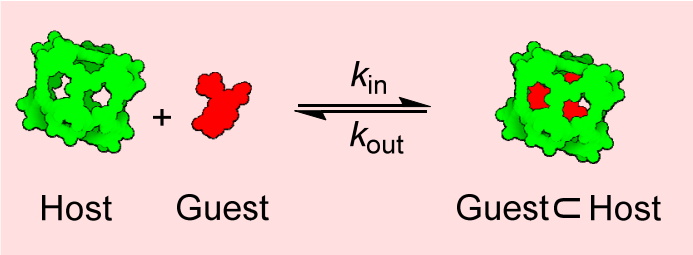
2. Materials and Methods

The molecular encapsulation kinetics and thermodynamics had been obtained using standard 1:1 host–guest binding isotherms. Simulations were performed using the R software [83] and the RStudio software interface [84]. Differential equations, corresponding to the host–guest kinetic models, were solved with library deSolve using the standard parameters [85]. The Eyring equation was used to convert the activation-free energy barriers into kinetic constants [86]. In the simulations described in the manuscript, the guest⊂cage complexes had been set up according to the simulation performed, i.e., fast or

slow equilibrium. For the systems in fast equilibrium described in Section 3.1, the initial concentrations of both the host and guest were set up. Then, the amount of the guest⊂cage complex formed was calculated using the corresponding host–guest binding equilibrium and the associated equilibrium constant. For the systems in slow equilibrium described in Section 3.2, the initial concentration of the guest⊂cage complex was set up, then, the guest release was quantified by solving the corresponding differential rate law equations.

3. Results and Discussion

To explore the effects of the dilution, the binding constant strength, and the guest in–out activation energy, we modeled the host–guest encapsulation process considering the in-and-out processes involved in the encapsulation equilibrium (Figure 4). The in-step of guest encapsulation involved the reaction between a guest molecule and a host molecule; the step of the guest release involved a dissociative mechanism creating an empty cavity. This was a reasonable assumption considering the large host cavity occupancy required by the guest [87–89]. The complex formation step was, therefore, a second-order reaction, while the dissociative mechanism for the decomplexation step was a first-order reaction, with the corresponding equations described in Figure 4.



Equilibrium constant

$$K_{Ass} = \frac{k_{in}}{k_{out}} = \frac{[Guest \subset Host]}{[Guest]\,[Host]}$$

Differential rate law

$$d[Guest]/dt = -k_{in}\,[Guest]\,[Host] + k_{out}\,[Guest \subset Host]$$

$$d[Host]/dt = -k_{in}\,[Guest]\,[Host] + k_{out}\,[Guest \subset Host]$$

$$d[Guest \subset Host]/dt = k_{in}\,[Guest]\,[Host] - k_{out}\,[Guest \subset Host]$$

Figure 4. Dissociative mechanism of a guest⊂host complex with the corresponding equilibrium constant and differential rate law for the reversible encapsulation reaction.

3.1. Effects of Dilution in Guest⊂Cage Complexes

A large number of the reported cage structures in the literature have sufficiently large portals that allow the fast entry and exit of guests from the cavity, allowing these systems to operate under equilibrium conditions at room temperature. These systems result in labile guest⊂cage complexes, where the guest can rapidly pass in–out of the cage. When the guest⊂cage complex is diluted, a re-equilibration takes place as dictated by the equilibrium constant, resulting in the guest escaping from the cage cavity. As the required concentrations for the biological experiments are usually in the micromolar range, this produces practically no significant binding, unless the binding constant is as high as 10^6 or 10^8 M^{-1}. Figure 5a shows the effect of the binding constant on the encapsulation equilibrium, for example, when $K_{Ass} = 10^8$ M^{-1} a 4% of the guest is released from the cage at 5 μM concentration, and nearly 40% if $K_{Ass} = 10^6$ M^{-1}. The amount of the encapsulated guest can be increased by using an excess concentration of the cage. According to the Le Chatelier principle, the excess of cages shifts the equilibrium towards the formation of the host–guest complex (Figure 5b). For example, when the association constant is 10^6 M^{-1} and the concentration of the guest is 5 μM, an increase in the cage concentration from 5 μM to 25 μM raises the amount of encapsulated guest from 60% to 95% (Figure 5a,b). Thus,

cages with a good affinity towards guests may be suitable for biological applications by using either equimolar amounts if the association constant is as high as 10^8 M^{-1}, or using an excess of cages to favor encapsulation. Note that these systems may be suitable for in vitro studies, as it is possible to set up the concentration in the well, but not suitable for in vivo studies, where additional dilution effects will occur. Therefore, to preserve the encapsulated guest in the guest⊂cage complex after dilution, it is necessary to develop systems with constrictive binding.

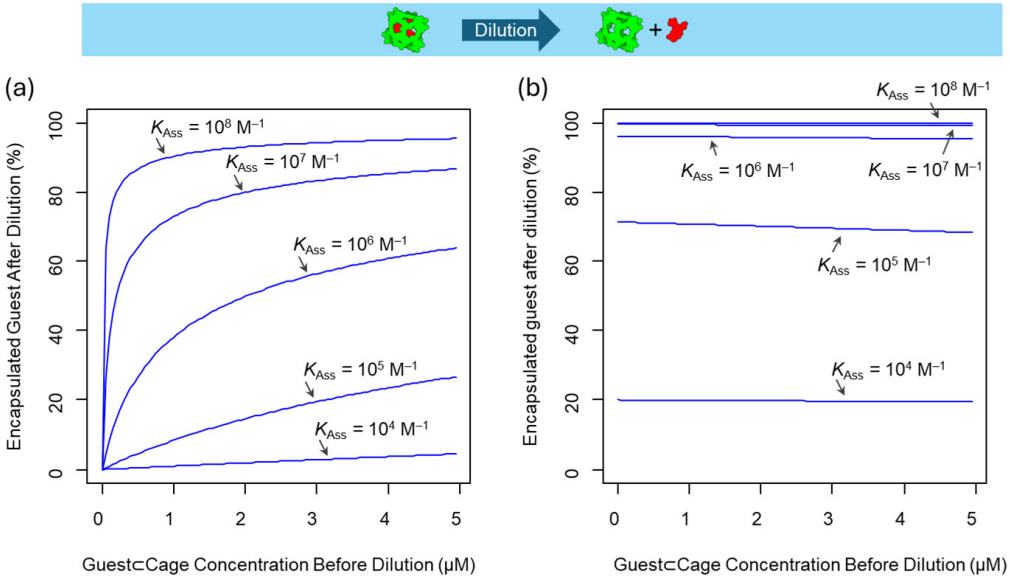


Figure 5. Percentage of encapsulated guest at different guest⊂cage concentrations after dilution considering different association constant values. (**a**) Dilution of a solution containing the guest⊂cage complex. (**b**) Dilution of a solution containing the guest⊂cage complex and an excess cage with a total cage concentration of 25 μM. K_{Ass} represents the guest–cage association constant. In the schematic representation of the guest, cage, and guest⊂cage complex, the guest is represented in red and the cage in green.

3.2. Energy Barrier for Guest Escaping the Cavity in Guest⊂Cage Complexes

To overcome the limitations of the guest⊂cage complexes that operate under equilibrium conditions, it is necessary to develop kinetically locked guest⊂cage systems, i.e., systems under constrictive binding. We had simulated the guest release from a guest⊂cage complex at different energy barriers and association constants considering an initial guest⊂cage concentration of 1 μM (Figure 6). When the association constant was as low as 10^3 M^{-1} and the guest–out activation barrier was 23 kcal/mol or lower, a complete release of the guest was achieved in less than 20 h (Figure 6a). If the association constant was 10^6 M^{-1}, a similar release in kinetic dependency with the guest–out activation barrier was observed (Figure 6b), but with a significant difference; in this case, the larger affinity resulted in a significant amount of the guest being encapsulated when the equilibrium was reached. These results show that guest⊂cage systems with a guest–out activation barrier of at least 25 kcal/mol are suitable for keeping 95% of the encapsulated guest for at least 10 h. These inert systems are ideal for achieving the required performance in biological applications, as they will not suffer from re-equilibration via dilution effects, making them suitable for in vivo studies.

The results from the simulations of Figure 6 demonstrate that guest⊂cage systems with an activation barrier of at least 25 kcal/mol for the guest exit are ideal "gate closed" systems, effectively keeping the guest inside the cage. Engineering the structure of cages with stimuli-responsive motifs results in a "gate closed"–"gate open" system for on-command guest release. In these systems, the encapsulated guest is not able to escape from the cavity of the cage in the "gate closed" system (i.e., large guest–out activation barrier) until a

certain stimulus is present that activates the "gate open" state (i.e., low guest–out activation barrier). See Figure 2 for examples of stimuli that trigger the "gate open" event. We have simulated the release of the guest from a guest⊂cage at the concentration of 1 μM with a guest–out activation barrier of 26 kcal/mol. The "gate open" event was introduced in the simulation by changing the energy barrier ($\Delta G^{\ddagger}_{out}$) at a specific time to simulate the chemical event that induced the gate opening. A minimal guest release was observed until the gate opening occurred in response to a specific stimulus that reduced the barrier to 23 kcal/mol (Figure 7). This change in the activation barrier led to complete guest release when the association constant was 10^3 M^{-1} (Figure 7a), and a 60% release when the association constant was 10^6 M^{-1}, due to the equilibrium reached between the host and guest (Figure 7b).

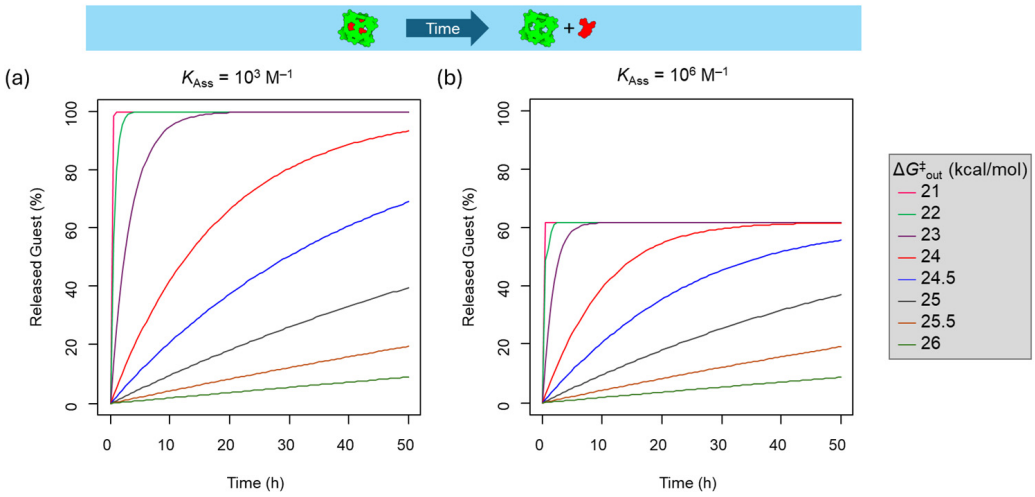


Figure 6. Guest release kinetics of from guest⊂cage complexes (1 μM) with different activation barriers for: (**a**) guest–cage association constant of 10^3 M^{-1}, (**b**) guest–cage association constant of 10^6 M^{-1}. $\Delta G^{\ddagger}_{out}$ represents guest–out activation barrier and K_{Ass} the guest–cage association constant. In the schematic representation of the guest, cage, and guest⊂cage complex, the guest is represented in red and the cage in green.

The "gate closed"–"gate open" systems are, therefore, ideal for biological applications due to their release properties. A last aspect to consider is the feasibility of preparing the guest⊂cage complex under chemical synthetic conditions. An effective guest⊂cage synthesis requires a high association constant to drive the formation of the host–guest complex. Therefore, from the synthetic point of view, an association constant of 10^6 M^{-1} would be preferred. However, as described in Figure 7b the high guest–cage affinity does not allow the complete release of the guest due to the encapsulation equilibrium. Developing a more sophisticated guest⊂cage system that simultaneously produces gate opening and affinity reduction in response to stimuli would be ideal. This can be achieved, for example, by partial or full cage disassembly (see Figure 2 for examples of stimuli that trigger the "gate open" event). We have simulated this, using the same conditions described in Figure 7, but adding to the reduction in the guest–out barrier in the "gate open" event a reduction in the association constant (Figure 8). The "gate open" event was introduced in the simulation by changing the energy barrier ($\Delta G^{\ddagger}_{out}$) and the association constant (K_{Ass}) at a certain time to simulate the chemical event that induced the gate opening with a reduction in the affinity towards the guest. This system has the ideal properties from a synthetic point of view, i.e., a high association constant that facilitates the guest⊂cage formation with a high out activation barrier that prevents the guest from escaping the cavity. Note that synthesis may require heating to achieve a suitable guest rate or to self-assemble the cage around the guest molecule. Then, when the gate is open, a reduction in both the guest–out energy barrier and the cage–guest affinity occurs, resulting in complete guest release. These guest⊂cage complexes have, therefore, ideal properties for in vivo studies.

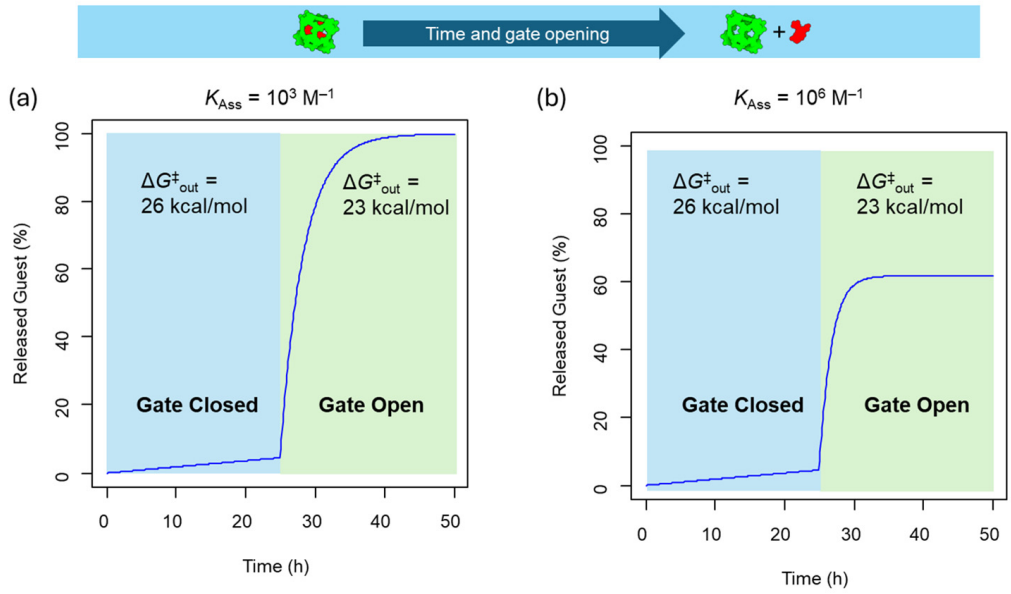


Figure 7. Guest release kinetics from guest⊂cage (1 μM) complexes with an activation barrier of 26 kcal/mol in the gate closed state that is reduced to 23 kcal/mol in the gate open state in response to a stimulus for: (**a**) guest–cage association constant of 10^3 M^{-1}, (**b**) guest–cage association constant of 10^6 M^{-1}. $\Delta G^{‡}_{out}$ represents guest–out activation barrier and K_{Ass} the guest–cage association constant. In the schematic representation of the guest, cage, and guest⊂cage complex, the guest is represented in red and the cage in green.

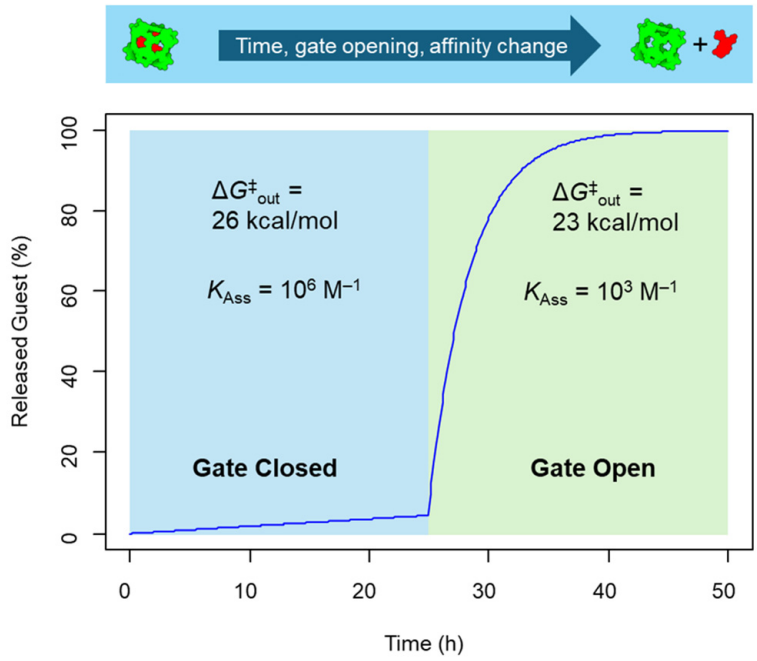


Figure 8. Guest release kinetics of guest⊂cage complexes (1 μM) with an activation barrier of 26 kcal/mol in the gate-closed state, which is reduced to 23 kcal/mol in the gate-open state in response to a stimulus, with the simultaneous reduction in the guest–cage association constant. $\Delta G^{‡}_{out}$ represents guest–out activation barrier. In the schematic representation of the guest, cage, and guest⊂cage complex, the guest is represented in red and the cage in green.

4. Conclusions

Molecular cages have excellent host–guest properties for drug delivery applications. We have shown that dynamic systems, in which the guest can rapidly pass in–out, can

result in a guest⊂cage complex suitable for drug delivery in vitro, with limitations for in vivo experiments due to guest release by dilution effects. These limitations are overcome with constrictive binding guest⊂cage complexes, where the guest is trapped in the cavity of the cage in a "gate closed" state. On-command guest release is therefore achieved by the "gate open" state, which produces a reduction in the guest–out energy barrier, allowing the release of the guest. A complete guest release is achieved when the gate-opening event also produces a reduction in the cage–guest affinity. As a result, this study shows that overall guest⊂cage complexes might have suitable properties for drug delivery in biological environments; yet, to achieve this goal, molecular cages with the necessary structures and properties to meet the required thermodynamic and kinetic criteria need to be designed. Future work in the field of molecular cages will soon enable the synthesis of molecular cages with constrictive binding of drug molecules with optimal properties for in vivo drug delivery.

Author Contributions: Conceptualization, V.M.-C.; methodology, G.M.-G. and V.M.-C.; experiments and simulations, V.M.-C. and G.M.-G.; writing—original draft preparation, G.M.-G., V.M.-C. and R.M.-M.; writing—review and editing, G.M.-G., V.M.-C. and R.M.-M.; supervision, V.M.-C. and R.M.-M.; project administration, V.M.-C. and R.M.-M.; funding acquisition, V.M.-C. and R.M.-M. All authors have read and agreed to the published version of the manuscript.

Funding: V.M.-C. acknowledges the financial support from project CIDEGENT/2020/031 funded by the Generalitat Valenciana, project PID2020-113256RA-I00 funded by MICIU/AEI/10.13039/501100011033, and project CNS2023-144879 funded by MICIU/AEI/10.13039/501100011033, and European Union NextGenerationEU/PRTR. R.M.-M. acknowledges the financial support from project PROMETEO CIPROM/2021/007 from the Generalitat Valenciana and project PID2021-126304OB-C41 funded by MICIU/AEI/10.13039/501100011033 and FEDER A way to make Europe.

Institutional Review Board Statement: Not applicable.

Informed Consent Statement: Not applicable.

Data Availability Statement: All data the generated or analyzed during this study are included in the manuscript. The original contributions presented in this study are included in the article; further inquiries can be directed to the corresponding authors.

Acknowledgments: This research was supported by CIBER (CB06/01/2012), Instituto de Salud Carlos III, Ministerio de Ciencia e Innovación.

Conflicts of Interest: The authors declare no conflicts of interest.

References

1. Montà-González, G.; Sancenón, F.; Martínez-Máñez, R.; Martí-Centelles, V. Purely Covalent Molecular Cages and Containers for Guest Encapsulation. *Chem. Rev.* **2022**, *122*, 13636–13708. [CrossRef] [PubMed]
2. Percástegui, E.G.; Ronson, T.K.; Nitschke, J.R. Design and Applications of Water-soluble Coordination Cages. *Chem. Rev.* **2020**, *120*, 13480–13544. [CrossRef] [PubMed]
3. Lewis, J.E.M. Developing Sophisticated Microenvironments in Metal-organic Cages. *Trends Chem.* **2023**, *5*, 717–719. [CrossRef]
4. Penocchio, E.; Bachir, A.; Credi, A.; Astumian, R.D.; Ragazzon, G. Analysis of Kinetic Asymmetry in a Multi-Cycle Reaction Network Establishes the Principles for Autonomous Compartmentalized Molecular Ratchets. *Chem* **2024**, *article in press*. [CrossRef]
5. Martí-Centelles, V.; Pandey, M.D.; Burguete, M.I.; Luis, S.V. Macrocyclization Reactions: The Importance of Conformational, Configurational, and Template-Induced Preorganization. *Chem. Rev.* **2015**, *115*, 8736–8834. [CrossRef]
6. Martí-Centelles, V.; Duarte, F.; Lusby, P.J. Host-Guest Chemistry of Self-Assembled Hemi-Cage Systems: The Dramatic Effect of Lost Pre-Organization. *Isr. J. Chem.* **2019**, *59*, 257–266. [CrossRef]
7. Chaudhuri, S.; Verderame, M.; Mako, T.L.; Bandara, Y.M.N.D.Y.; Fernando, A.I.; Levine, M. Synthetic B-cyclodextrin Dimers for Squaraine Binding: Effect of Host Architecture on Photophysical Properties, Aggregate Formation and Chemical Reactivity. *Eur. J. Org. Chem.* **2018**, *2018*, 1964–1974. [CrossRef]
8. Martí-Centelles, V.; Lawrence, A.L.; Lusby, P.J. High Activity and Efficient Turnover by a Simple, Self-Assembled Artificial "Diels-Alderase". *J. Am. Chem. Soc.* **2018**, *140*, 2862–2868. [CrossRef]
9. Pappalardo, A.; Puglisi, R.; Trusso Sfrazzetto, G. Catalysis inside Supramolecular Capsules: Recent Developments. *Catalysts* **2019**, *9*, 630. [CrossRef]

10. Piskorz, T.K.; Martí-Centelles, V.; Spicer, R.L.; Duarte, F.; Lusby, P.J. Picking the Lock of Coordination Cage Catalysis. *Chem. Sci.* **2023**, *14*, 11300–11331. [CrossRef]
11. Ward, M.D. New Insights into Coordination-cage Based Catalysis. *Chem. Commun.* **2024**, *60*, 10464–10475. [CrossRef] [PubMed]
12. Andrews, K.G.; Piskorz, T.K.; Horton, P.N.; Coles, S.J. Enzyme-like Acyl Transfer Catalysis in a Bifunctional Organic Cage. *J. Am. Chem. Soc.* **2024**, *146*, 17887–17897. [CrossRef] [PubMed]
13. Luo, K.; Liu, Y.; Li, A.; Lai, Z.; Long, Z.; He, Q. A Tetraphenylethylene-Based Superphane for Selective Detection and Adsorption of Trace Picric Acid in Aqueous Media. *Supramol. Chem.* **2024**, *article in press*. [CrossRef]
14. La Cognata, S.; Amendola, V. Recent Applications of Organic Cages in Sensing and Separation Processes in Solution. *Chem. Commun.* **2023**, *59*, 13668–13678. [CrossRef] [PubMed]
15. Merli, D.; La Cognata, S.; Balduzzi, F.; Miljkovic, A.; Toma, L.; Amendola, V. A Smart Supramolecular Device for the Detection of *t*,*t*-Muconic Acid in Urine. *New J. Chem.* **2018**, *42*, 15460–15465. [CrossRef]
16. Ludden, M.D.; Taylor, C.G.P.; Ward, M.D. Orthogonal Binding and Displacement of Different Guest Types Using a Coordination Cage Host with Cavity-Based and Surface-Based Binding Sites. *Chem. Sci.* **2021**, *12*, 12640–12650. [CrossRef]
17. Lu, Y.; Wang, S.-M.; He, S.-S.; Huang, Q.; Zhao, C.-D.; Yu, S.; Jiang, W.; Yao, H.; Wang, L.-L.; Yang, L.-P. An Endo-functionalized Molecular Cage for Selective Potentiometric Determination of Creatinine. *Chem. Sci.* **2024**, *14*, 14791–14797. [CrossRef]
18. Maitra, P.K.; Bhattacharyya, S.; Purba, P.C.; Mukherjee, P.S. Coordination-induced Emissive Poly-nhc-derived Metallacage for Pesticide Detection. *Inorg. Chem.* **2024**, *63*, 2569–2576. [CrossRef]
19. Zhang, D.; Ronson, T.K.; Zou, Y.-Q.; Nitschke, J.R. Metal–organic Cages for Molecular Separations. *Nat. Rev. Chem.* **2021**, *5*, 168–182. [CrossRef]
20. Little, M.A.; Cooper, A.I. The Chemistry of Porous Organic Molecular Materials. *Adv. Funct. Mater.* **2020**, *30*, 1909842. [CrossRef]
21. Zhang, J.; Xie, S.; Zi, M.; Yuan, L. Recent Advances of Application of Porous Molecular Cages for Enantioselective Recognition and Separation. *J. Sep. Sci.* **2020**, *43*, 134–149. [CrossRef] [PubMed]
22. García-Simón, C.; Garcia-Borràs, M.; Gómez, L.; Parella, T.; Osuna, S.; Juanhuix, J.; Imaz, I.; Maspoch, D.; Costas, M.; Ribas, X. Sponge-like Molecular Cage for Purification of Fullerenes. *Nat. Commun.* **2014**, *5*, 5557. [CrossRef] [PubMed]
23. Ghosh, A.; Pruchyathamkorn, J.; Fuertes Espinosa, C.; Nitschke, J.R. Light-driven Purification of Progesterone from Steroid Mixtures Using a Photoresponsive Metal–organic Capsule. *J. Am. Chem. Soc.* **2024**, *146*, 2568–2573. [CrossRef]
24. Pérez-Ferreiro, M.; Gallagher, Q.M.; León, A.B.; Webb, M.A.; Criado, A.; Mosquera, J. Engineering a Surfactant Trap via Postassembly Modification of an Imine Cage. *Chem. Mater.* **2024**, *36*, 8920–8928. [CrossRef] [PubMed]
25. Wang, Z.; Pacheco-Fernández, I.; Carpenter, J.E.; Aoyama, T.; Huang, G.; Pournaghshband Isfahani, A.; Ghalei, B.; Sivaniah, E.; Urayama, K.; Colón, Y.J.; et al. Pore-networked Membrane Using Linked Metal-organic Polyhedra for Trace-level Pollutant Removal and Detection in Environmental Water. *Commun. Mater.* **2024**, *5*, 161. [CrossRef]
26. Samanta, J.; Tang, M.; Zhang, M.; Hughes, R.P.; Staples, R.J.; Ke, C. Tripodal Organic Cages with Unconventional CH···O Interactions for Perchlorate Remediation in Water. *J. Am. Chem. Soc.* **2023**, *145*, 21723–21728. [CrossRef]
27. Liu, X.; Zhang, Z.; Shui, F.; Zhang, S.; Li, L.; Wang, J.; Yi, M.; You, Z.; Yang, S.; Yang, R.; et al. Porous Organic Cage as an Efficient Platform for Industrial Radioactive Iodine Capture. *Angew. Chem. Int. Ed.* **2024**, *63*, e202411342. [CrossRef]
28. Mal, P.; Breiner, B.; Rissanen, K.; Nitschke, J.R. White Phosphorus is Air-Stable within a Self-Assembled Tetrahedral Capsule. *Science* **2009**, *324*, 1697–1699. [CrossRef]
29. Galan, A.; Ballester, P. Stabilization of Reactive Species by Supramolecular Encapsulation. *Chem. Soc. Rev.* **2016**, *45*, 1720–1737. [CrossRef]
30. Montà-González, G.; Ortiz-Gómez, E.; López-Lima, R.; Fiorini, G.; Martínez-Máñez, R.; Martí-Centelles, V. Water-Soluble Molecular Cages for Biological Applications. *Molecules* **2024**, *29*, 1621. [CrossRef]
31. Tapia, L.; Alfonso, I.; Solà, J. Molecular Cages for Biological Applications. *Org. Biomol. Chem.* **2021**, *19*, 9527–9540. [CrossRef] [PubMed]
32. Casini, A.; Woods, B.; Wenzel, M. The Promise of Self-Assembled 3D Supramolecular Coordination Complexes for Biomedical Applications. *Inorg. Chem.* **2017**, *56*, 14715–14729. [CrossRef] [PubMed]
33. Montà-González, G.; Bastante-Rodríguez, D.; García-Fernández, A.; Lusby, P.J.; Martínez-Máñez, R.; Martí-Centelles, V. Comparing organic and metallo-organic hydrazone molecular cages as potential carriers for doxorubicin delivery. *Chem. Sci.* **2024**, *15*, 10010–10017. [CrossRef] [PubMed]
34. Sun, D.; Feng, X.; Zhu, X.; Wang, Y.; Yang, J. Anticancer Agents Based on Metal Organic Cages. *Coord. Chem. Rev.* **2024**, *500*, 215546. [CrossRef]
35. Dou, W.-T.; Yang, C.-Y.; Hu, L.-R.; Song, B.; Jin, T.; Jia, P.-P.; Ji, X.; Zheng, F.; Yang, H.-B.; Xu, L. Metallacages and Covalent Cages for Biological Imaging and Therapeutics. *ACS Mater. Lett.* **2023**, *5*, 1061–1082. [CrossRef]
36. Tapia, L.; Pérez, Y.; Carreira-Barral, I.; Bujons, J.; Bolte, M.; Bedia, C.; Solà, J.; Quesada, R.; Alfonso, I. Tuning pH-dependent Cytotoxicity in Cancer Cells by Peripheral Fluorine Substitution on Pseudopeptidic Cages. *Cell Rep. Phys. Sci.* **2024**, *5*, 102152. [CrossRef]
37. Mosquera, J.; Henriksen-Lacey, M.; García, I.; Martínez-Calvo, M.; Rodríguez, J.; Mascareñas, J.L.; Liz-Marzán, L.M. Cellular Uptake of Gold Nanoparticles Triggered by Host–Guest Interactions. *J. Am. Chem. Soc.* **2018**, *140*, 4469–4472. [CrossRef]
38. Rodríguez, J.; Mosquera, J.; Couceiro, J.R.; Nitschke, J.R.; Vázquez, M.E.; Mascareñas, J.L. Anion Recognition as a Supramolecular Switch of Cell Internalization. *J. Am. Chem. Soc.* **2017**, *139*, 55–58. [CrossRef]

39. Hernández-López, L.; Von Baeckmann, C.; Martínez-Esaín, J.; Cortés-Martínez, A.; Faraudo, J.; Caules, C.; Parella, T.; Maspoch, D.; Carné-Sánchez, A. (Bio)functionalisation of Metal–organic Polyhedra by Using Click Chemistry. *Chem. Eur. J.* **2023**, *29*, e202301945. [CrossRef]
40. Ling, Q.-H.; Lou, Z.-C.; Zhang, L.; Jin, T.; Dou, W.-T.; Yang, H.-B.; Xu, L. Supramolecular Cage-mediated Cargo Transport. *Chem. Soc. Rev.* **2024**, *53*, 6042–6067. [CrossRef]
41. Nakabayashi, K.; Kawano, M.; Fujita, M. pH-Switchable Through-Space Interaction of Organic Radicals within a Self-Assembled Coordination Cage. *Angew. Chem. Int. Ed.* **2005**, *44*, 5322–5325. [CrossRef] [PubMed]
42. Sivalingam, V.; Parbin, M.; Krishnaswamy, S.; Chand, D.K. Cage-to-Cage Transformations in Self-Assembled Coordination Cages Using "Acid/Base" or "Guest Binding-Induced Strain" as Stimuli. *Angew. Chem. Int. Ed.* **2024**, *63*, e202403711. [CrossRef] [PubMed]
43. Benchimol, E.; Tessarolo, J.; Clever, G.H. Photoswitchable Coordination Cages. *Nat. Chem.* **2024**, *16*, 13–21. [CrossRef] [PubMed]
44. Lee, H.; Tessarolo, J.; Langbehn, D.; Baksi, A.; Herges, R.; Clever, G.H. Light-Powered Dissipative Assembly of Diazocine Coordination Cages. *J. Am. Chem. Soc.* **2022**, *144*, 3099–3105. [CrossRef] [PubMed]
45. DiNardi, R.G.; Douglas, A.O.; Tian, R.; Price, J.R.; Tajik, M.; Donald, W.A.; Beves, J.E. Visible-Light-Responsive Self-Assembled Complexes: Improved Photoswitching Properties by Metal Ion Coordination. *Angew. Chem. Int. Ed.* **2022**, *61*, e202205701. [CrossRef]
46. Kennedy, A.D.W.; DiNardi, R.G.; Fillbrook, L.L.; Donald, W.A.; Beves, J.E. Visible-Light Switching of Metallosupramolecular Assemblies. *Chem. Eur. J.* **2022**, *28*, e202104461. [CrossRef]
47. Lewis, J.E.M.; Gavey, E.L.; Cameron, S.A.; Crowley, J.D. Stimuli-responsive Pd_2L_4 metallosupramolecular Cages: Towards Targeted Cisplatin Drug Delivery. *Chem. Sci.* **2012**, *3*, 778–784. [CrossRef]
48. Clegg, J.K.; Cremers, J.; Hogben, A.J.; Breiner, B.; Smulders, M.M.J.; Thoburn, J.D.; Nitschke, J.R. A Stimuli Responsive System of Self-assembled Anion-binding $Fe_4L_6^{8+}$ cages. *Chem. Sci.* **2013**, *4*, 68–76. [CrossRef]
49. Vasdev, R.A.S.; Findlay, J.A.; Garden, A.L.; Crowley, J.D. Redox Active $[Pd_2L_4]^{4+}$ Cages Constructed from Rotationally Flexible 1,10-Disubstituted Ferrocene Ligands. *Chem. Commun.* **2019**, *55*, 7506–7509. [CrossRef]
50. Lisboa, L.S.; Findlay, J.A.; Wright, L.J.; Hartinger, C.G.; Crowley, J.D. A Reduced-Symmetry Heterobimetallic $[PdPtL_4]^{4+}$ Cage: Assembly, Guest Binding, and Stimulus-Induced Switching. *Angew. Chem. Int. Ed.* **2020**, *59*, 11101–11107. [CrossRef]
51. Barber, B.E.; Jamieson, E.M.G.; White, L.E.M.; Mcternan, C.T. Metal-peptidic Cages—Helical Oligoprolines Generate Highly Anisotropic Nanospaces with Emergent Isomer Control. *Chem* **2024**, *10*, 2792–2806. [CrossRef]
52. Liu, Y.; Liu, F.-Z.; Li, S.; Wang, P.; Wang, J.; Chu, Z.; Zhang, Z.; Yan, K. Guest Release from Coordination Assemblies in the Solid State. *Chem* **2024**, *10*, 1502–1515. [CrossRef]
53. Martí-Centelles, V. Kinetic and thermodynamic concepts as synthetic tools in supramolecular chemistry for preparing macrocycles and molecular cages. *Tetrahedron Lett.* **2022**, *93*, 153676. [CrossRef]
54. Lewis, J.E.M. Molecular Engineering of Confined Space in Metal–organic Cages. *Chem. Commun.* **2022**, *58*, 13873–13886. [CrossRef] [PubMed]
55. Yang, X.; Ullah, Z.; Stoddart, J.F.; Yavuz, C.T. Porous Organic Cages. *Chem. Rev.* **2023**, *123*, 4602–4634. [CrossRef]
56. Martí-Centelles, V.; Piskorz, T.K.; Duarte, F. CageCavityCalc (*C3*): A Computational Tool for Calculating and Visualizing Cavities in Molecular Cages. *J. Chem. Inf. Model.* **2024**, *64*, 5604–5616. [CrossRef]
57. Piskorz, T.K.; Martí-Centelles, V.; Young, T.A.; Lusby, P.J.; Duarte, F. Computational Modeling of Supramolecular Metallo-organic Cages-Challenges and Opportunities. *ACS Catal.* **2022**, *12*, 5806–5826. [CrossRef]
58. Tarzia, A.; Wolpert, E.H.; Jelfs, K.E.; Pavan, G.M. Systematic Exploration of Accessible Topologies of Cage Molecules via Minimalistic Models. *Chem. Sci.* **2023**, *14*, 12506–12517. [CrossRef]
59. Young, T.A.; Gheorghe, R.; Duarte, F. cgbind: A Python Module and Web App for Automated Metallocage Construction and Host–Guest Characterization. *J. Chem. Inf. Model.* **2020**, *60*, 3546–3557. [CrossRef]
60. Turcani, L.; Tarzia, A.; Szczypiński, F.T.; Jelfs, K.E. stk: An Extendable Python Framework for Automated Molecular and Supramolecular Structure Assembly and Discovery. *J. Chem. Phys.* **2021**, *154*, 214102. [CrossRef]
61. Santolini, V.; Miklitz, M.; Berardo, E.; Jelfs, K.E. Topological Landscapes of Porous Organic Cages. *Nanoscale* **2017**, *9*, 5280–5298. [CrossRef] [PubMed]
62. Greenaway, R.L.; Jelfs, K.E. High-throughput Approaches for the Discovery of Supramolecular Organic Cages. *ChemPlusChem* **2020**, *85*, 1813–1823. [CrossRef]
63. Yang, Y.; Ronson, T.K.; Teeuwen, P.C.P.; Du, Y.; Zheng, J.; Wales, D.J.; Nitschke, J.R. Guest Binding Is Governed by Multiple Stimuli in Low-symmetry Metal-organic Cages Containing Bis-pyridyl(imine) Vertices. *Chem* **2024**, *article in press*. [CrossRef]
64. Gunawardana, V.W.L.; Ward, C.; Wang, H.; Holbrook, J.H.; Sekera, E.R.; Cui, H.; Hummon, A.B.; Badjić, J.D. Crystalline Nanoparticles of Water-Soluble Covalent Basket Cages (CBCs) for Encapsulation of Anticancer Drugs. *Angew. Chem. Int. Ed.* **2023**, *62*, e202306722. [CrossRef] [PubMed]
65. Conn, M.M.; Rebek, J., Jr. Self-Assembling Capsules. *Chem. Rev.* **1997**, *97*, 1647–1668. [CrossRef] [PubMed]
66. Quan, M.L.C.; Knobler, C.B.; Cram, D.J. Constrictive Binding by an Octalactone Hemicarcerand. *J. Chem. Soc. Chem. Commun.* **1991**, 660–662. [CrossRef]
67. Bobbins, T.A.; Cram, D.J. Comparisons of Activation Energies for Guest Escapes from the Inner Phases of Hemicarcerands with Varying Numbers of Bowl-linking Groups. *J. Chem. Soc., Chem. Commun.* **1995**, *15*, 1515–1516. [CrossRef]

68. Sheu, C.; Houk, K.N. Molecular Mechanics and Statistical Thermodynamics Studies of Complexes of a Flexible Hemicarcerand with Neutral Guests. *J. Am. Chem. Soc.* **1996**, *118*, 8056–8070. [CrossRef]
69. Smulders, M.M.J.; Zarra, S.; Nitschke, J.R. Quantitative Understanding of Guest Binding Enables the Design of Complex Host–guest Behavior. *J. Am. Chem. Soc.* **2013**, *135*, 7039–7046. [CrossRef]
70. Cram, D.J.; Jaeger, R.; Deshayes, K. Host-Guest Complexation. 65. Hemicarcerands that Encapsulate Hydrocarbons with Molecular Weights Greater than Two Hundred. *J. Am. Chem. Soc.* **1993**, *115*, 9879–10470. [CrossRef]
71. He, S.; Quan, M.; Yang, L.-P.; Au-Yeung, H.Y.; Jiang, W. Kinetic–thermodynamic Correlation of Conformational Changes in Ammonium Complexes of a Flexible Naphthocage. *Chem. Sci.* **2024**, *15*, 15841–15848. [CrossRef] [PubMed]
72. Liu, F.; Helgeson, R.C.; Houk, K.N. Building on Cram's Legacy: Stimulated Gating in Hemicarcerands. *Acc. Chem. Res.* **2014**, *47*, 2168–2176. [CrossRef] [PubMed]
73. Houk, K.N.; Nakamura, K.; Sheu, C.; Keating, A.E. Gating as a Control Element in Constrictive Binding and Guest Release by Hemicarcerands. *Science* **1996**, *273*, 627–629. [CrossRef] [PubMed]
74. Wang, H.; Liu, F.; Helgeson, R.C.; Houk, K.N. Reversible Photochemically Gated Transformation of a Hemicarcerand to a Carcerand. *Angew. Chem. Int. Ed.* **2013**, *52*, 655–659. [CrossRef] [PubMed]
75. Piatnitski, E.L.; Deshayes, K.D. Hemicarceplexes That Release Guests upon Irradiation. *Angew. Chem. Int. Ed.* **1998**, *37*, 970–972. [CrossRef]
76. Sun, J.; Patrick, B.O.; Sherman, J.C. A New [4]Carceplex, and a Crystal Structure and Dynamic Combinatorial Chemistry of a [5]Carceplex. *Tetrahedron* **2009**, *65*, 7296–7302. [CrossRef]
77. Helgeson, R.C.; Hayden, A.E.; Houk, K.N. Controlled Gating of a Hemicarcerand by Disulfide–Dithiol Interchange. *J. Org. Chem.* **2010**, *75*, 570–575. [CrossRef]
78. Escobar, L.; Escudero-Adán, E.C.; Ballester, P. Guest Exchange Mechanisms in Mono-Metallic Pd^{II}/Pt^{II}-Cages Based on a Tetra-Pyridyl Calix[4]pyrrole Ligand. *Angew. Chem. Int. Ed.* **2019**, *131*, 14277–14281. [CrossRef]
79. Rieth, S.; Hermann, K.; Wang, B.-Y.; Badjić, J.D. Controlling the Dynamics of Molecular Encapsulation and Gating. *Chem. Soc. Rev.* **2011**, *40*, 1609–1622. [CrossRef]
80. Ro, S.; Rowan, S.J.; Pease, A.R.; Cram, D.J.; Stoddart, J.F. Dynamic Hemicarcerands and Hemicarceplexes. *Org. Lett.* **2000**, *2*, 2411–2414. [CrossRef]
81. Yoshizawa, M.; Kusukawa, T.; Fujita, M.; Yamaguchi, K. Ship-in-a-bottle Synthesis of Otherwise Labile Cyclic Trimers of Siloxanes in a Self-assembled Coordination Cage. *J. Am. Chem. Soc.* **2000**, *122*, 6311–6312. [CrossRef]
82. Davis, A.V.; Raymond, K.N. The Big Squeeze: Guest Exchange in an M_4L_6 Supramolecular Host. *J. Am. Chem. Soc.* **2005**, *127*, 7912–7919. [CrossRef] [PubMed]
83. R Core Team. *R: A Language and Environment for Statistical Computing*, Version 4.0.5; R Foundation for Statistical Computing: Vienna, Austria, 2021. Available online: https://www.R-project.org/ (accessed on 16 September 2024).
84. RStudio Team. *RStudio: Integrated Development for R*, Version 2022.02.3; RStudio, Inc.: Boston, MA, USA, 2022. Available online: http://www.rstudio.com/ (accessed on 16 September 2024).
85. Soetaert, K.; Petzoldt, T.; Setzer, R.W. Solving Differential Equations in R: Package deSolve. *J. Statist. Soft.* **2010**, *33*, 1–25. [CrossRef]
86. Eyring, H. The Activated Complex in Chemical Reactions. *J. Chem. Phys.* **1935**, *3*, 107–115. [CrossRef]
87. Gibb, C.L.D.; Li, X.; Gibb, B.C. Adjusting the Binding Thermodynamics, Kinetics, and Orientation of Guests Within Large Synthetic Hydrophobic Pockets. *Proc. Natl. Acad. Sci. USA* **2002**, *99*, 4857–4862. [CrossRef]
88. Norjmaa, G.; Vidossich, P.; Maréchal, J.-D.; Ujaque, G. Modeling Kinetics and Thermodynamics of Guest Encapsulation into the $[M_4L_6]^{12-}$ Supramolecular Organometallic Cage. *J. Chem. Infor. Model.* **2021**, *61*, 4370–4381. [CrossRef]
89. Prabodh, A.; Sinn, S.; Grimm, L.; Miskolczy, Z.; Megyesi, M.; Biczók, L.; Bräse, S.; Biedermann, F. Teaching Indicators to Unravel the Kinetic Features of Host–guest Inclusion Complexes. *Chem. Commun.* **2020**, *56*, 12327–12330. [CrossRef]

Disclaimer/Publisher's Note: The statements, opinions and data contained in all publications are solely those of the individual author(s) and contributor(s) and not of MDPI and/or the editor(s). MDPI and/or the editor(s) disclaim responsibility for any injury to people or property resulting from any ideas, methods, instructions or products referred to in the content.